

Cold, clumpy accretion toward an active supermassive black hole

Grant R. Tremblay^{1,2,†}, J. B. Raymond Oonk^{3,4}, Françoise Combes⁵, Philippe Salomé⁵, Christopher O’Dea^{6,7}, Stefi A. Baum^{6,8}, G. Mark Voit⁹, Megan Donahue⁹, Brian R. McNamara¹⁰, Timothy A. Davis^{11,2,‡}, Michael A. McDonald¹², Alastair C. Edge¹³, Tracy E. Clarke¹⁴, Roberto Galván-Madrid^{15,2}, Malcolm N. Bremer¹⁶, Louise O. V. Edwards¹, Andrew C. Fabian¹⁷, Stephen Hamer⁵, Yuan Li¹⁸, Anaëlle Maury¹⁹, Helen Russell¹⁷, Alice C. Quillen²⁰, C. Megan Urry¹, Jeremy S. Sanders²¹, Michael Wise³

Supermassive black holes in galaxy centres can grow by the accretion of gas, liberating enormous amounts of energy that might regulate star formation on galaxy-wide scales^{1–3}. The nature of gaseous fuel reservoirs that power black hole growth is nevertheless largely unconstrained by observations, and is instead routinely simplified as a smooth, spherical inflow of very hot gas in accordance with the Bondi solution⁴. Recent theory^{5–7} and simulations^{8–10} instead predict that accretion can be dominated by a stochastic, clumpy distribution of very cold molecular clouds, though unambiguous observational support for this prediction remains elusive. Here we show observational evidence for a cold, clumpy accretion flow toward a supermassive black hole fuel reservoir in the nucleus of the Abell 2597 Brightest Cluster Galaxy (BCG), a nearby ($z = 0.0821$) giant elliptical galaxy surrounded by a dense halo of hot plasma^{11–13}. Under the right conditions, thermal instabilities can precipitate from this hot gas, producing a rain of cold clouds that fall toward the galaxy’s centre¹⁴, sustaining star formation amid a kiloparsec-scale molecular nebula that inhabits its core¹⁵. New interferometric sub-millimetre observations show that these cold clouds also fuel black hole accretion, revealing “shadows” cast by molecular clouds as they move inward at ~ 300 km s^{−1} toward the active supermassive black hole in the galaxy centre, which serves as a bright backlight. Corroborating evidence from prior observations¹⁶ of warmer atomic gas at extremely high spatial resolution¹⁷, along with simple arguments based on geometry and probability, indicates that these clouds are within the innermost hundred parsecs of the black hole, and falling closer toward it.

We observed the Abell 2597 Brightest Cluster Galaxy (Fig. 1) with the Atacama Large Millimeter/submillimeter Array (ALMA), enabling us to create a three-dimensional map of both the location and motions of cold gas at uniquely high sensitivity and spatial resolution. The ALMA receivers were sensitive to emission from the $J = 2 - 1$ rotational line of the carbon monoxide (CO) molecule. CO(2-1) emission is used as a tracer of cold ($\sim 10 - 30$ K) molecular hydrogen, which is vastly more abundant, but not directly observable at these low temperatures.

The continuum-subtracted CO(2-1) images (Fig. 2) reveal that the filamentary emission line nebula that spans the galaxy’s innermost ~ 30 kpc (Fig. 1b) consists not only of warm ionised gas^{18–20}, but cold molecular gas as well. In projection, the optical emission line nebula is cospatial and morphologically matched with CO(2-1) emission detected at a significance between $\gtrsim 3\sigma$ (in the outer filaments) and $\gtrsim 20\sigma$ (in the nuclear region) above the background noise level. The warm ionised nebula is therefore likely to have a substantial molecular component, consistent with results for other similar galaxies²¹. The total measured CO(2-1) line flux corresponds to a molecular hydrogen gas mass of $M_{\text{H}_2} = (1.8 \pm 0.2) \times 10^9 M_{\odot}$, where M_{\odot} is the mass of the sun. The critical (minimum) density for CO(2-1) emission requires that the volume filling factor of this gas be very low, of order a few percent. The projected spatial coincidence of both the warm ionised and cold molecular nebulae therefore supports the long-envisaged hypothesis that the ionised gas is merely the warm “skin” surrounding far colder and more massive molecular cores^{22,23}, whose outer regions are heated by intense radiation from the environment in which they reside. Rather than a monolithic, kiloparsec-scale slab of cold gas, we are more likely observing a projected superposition of many smaller, isolated clouds and filaments.

The data unambiguously show that cold molecular gas is falling inward along a line of sight that intersects the galaxy centre. We know this because the ALMA beam cospatial with the millimetre continuum source, the radio core, and the isophotal centre of the galaxy reveals strong, redshifted continuum absorption (Fig. 3b), found by extracting the CO(2-1) spectrum from this central beam. This reveals at least three deep and narrow absorption lines (Fig. 3c), with redshifted line centres at +240, +275, and +335 km s^{−1} relative to the systemic (stellar) velocity of the galaxy, all within an angular (physical) region of $0''.715 \times 0''.533$ (1 kpc \times 0.8 kpc).

These absorption features arise from cold molecular clouds moving toward the centre of the galaxy, either via radial or inspiralling trajectories. They manifest as continuum absorption because they cast “shadows” along the line of sight as the clouds eclipse or attenuate about 20% (or about 2 mJy) of the millimetre synchrotron continuum

¹Yale Center for Astronomy & Astrophysics, Yale University, 52 Hillhouse Ave., New Haven, CT 06511, USA ²European Southern Observatory, Karl-Schwarzschild-Str. 2, 85748, Garching bei München, Germany ³ASTRON, Netherlands Institute for Radio Astronomy, P.O. Box 2, 7990 AA Dwingeloo, The Netherlands ⁴Leiden Observatory, Leiden University, Niels Borhweg 2, NL-2333 CA Leiden, The Netherlands ⁵LERMA, Observatoire de Paris, PSL Research Univ., Collège de France, CNRS, Sorbonne Univ., Paris, France ⁶Department of Physics & Astronomy, University of Manitoba, Winnipeg, MB R3T 2N2, Canada ⁷School of Physics & Astronomy, Rochester Institute of Technology, 84 Lomb Memorial Dr., Rochester, NY 14623, USA ⁸Chester F. Carlson Center for Imaging Science, Rochester Institute of Technology, 84 Lomb Memorial Dr., Rochester, NY 14623, USA ⁹Physics & Astronomy Department, Michigan State University, East Lansing, MI 48824-2320, USA ¹⁰Physics & Astronomy Department, Waterloo University, 200 University Ave. W., Waterloo, ON, N2L 2G1, Canada ¹¹School of Physics & Astronomy, Cardiff University, The Parade, Cardiff CF24 3AA, United Kingdom ¹²Kavli Institute for Astrophysics & Space Research, MIT, 77 Massachusetts Ave., Cambridge, MA 02139, USA ¹³Department of Physics, Durham University, Durham, DH1 3LE, United Kingdom ¹⁴Naval Research Laboratory Remote Sensing Division, Code 7213 4555 Overlook Ave. SW, Washington, DC 20375, USA ¹⁵Instituto de Radioastronomía y Astrofísica, UNAM, Apdo. Postal 3-72 (Xangari), 58089 Morelia, Michoacán, México ¹⁶H. W. Wills Physics Laboratory, University of Bristol, Tyndall Avenue, Bristol, BS8 1TL, United Kingdom ¹⁷Institute of Astronomy, Cambridge University, Madingley Rd., Cambridge, CB3 0HA, United Kingdom ¹⁸Department of Astronomy, University of Michigan, 1085 S. University Avenue, Ann Arbor, MI 48109, USA ¹⁹Laboratoire AIM-Paris-Saclay, CEA/DSM/Ifu CNRS ? Univ. Paris Diderot, CE-Saclay, F-91191 Gif-sur-Yvette, France ²⁰Department of Physics & Astronomy, University of Rochester, Rochester, NY 14627, USA ²¹Max Planck Institut für Extraterrestrische Physik, 85748 Garching bei München, Germany

[†] Einstein Fellow [‡] Rutherford Fellow

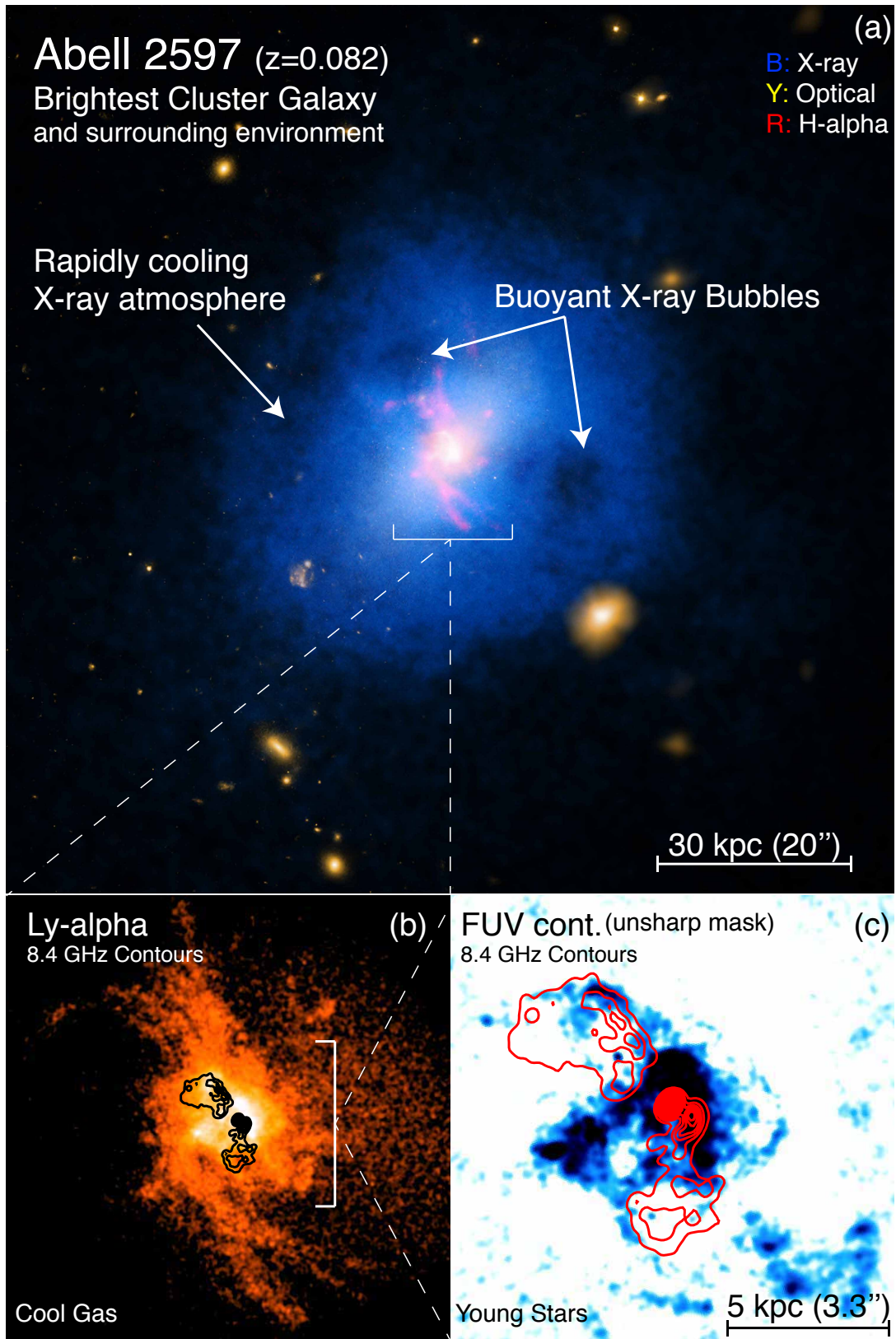


Figure 1 | A multiwavelength view of the Abell 2597 BCG. (a) *Chandra* X-ray, *HST* and DSS optical, and Magellan $H\alpha+[NII]$ emission is shown in blue, yellow, and red, respectively (Credit: X-ray: NASA / CXC / Michigan State Univ / G.Voit et al; Optical: NASA/STScI & DSS; $H\alpha$: Carnegie Obs. / Magellan / W.Baade Telescope / U.Maryland / M.McDonald). (b) *HST* image of $Ly\alpha$ emission associated with the ionised gas nebula 13. (c) Unsharp mask of the *HST* far-ultraviolet continuum image of the central regions of the nebula¹³. Very Large Array (VLA) radio contours of the 8.4 GHz source are overlaid in red.

source, which serves as a bright backlight (13.6 mJy at rest-frame 230 GHz). The synchrotron continuum is emitted by jets launched from the accreting supermassive ($\sim 3 \times 10^8 M_\odot$)¹³ black hole in the galaxy’s active nucleus (Fig. 4). The absorbers must therefore be located somewhere between the observer and the galaxy centre, falling deeper into the galaxy at $\sim +300 \text{ km s}^{-1}$ toward the black hole at its core. This radial speed is roughly equal to the expected circular velocity²⁴ in the nucleus, consistent either with a nearly radial orbit, or highly non-circular motions in close proximity to the galaxy’s core.

Gaussian fits to the spectral absorption features reveal narrow linewidths of $\sigma \lesssim 6 \text{ km s}^{-1}$, which means the absorbers are more likely spatially compact, with sizes that span tens (rather than hundreds or thousands) of parsecs. The shapes of the absorption lines remain roughly the same regardless of how finely the spectra are binned, suggesting that the absorbers are likely coherent structures, rather than a superposition of many smaller absorbers unresolved in velocity space. If each absorption feature corresponds to one coherent cloud, and if those clouds roughly obey size-linewidth relations^{25,26} for giant molecular clouds in the Milky Way, they should have diameters not larger than $\sim 40 \text{ pc}$. If in virial equilibrium, molecular clouds this size would have masses of order $10^{5-6} M_\odot$, and if in rough pressure equilibrium with their ambient multiphase 10^{3-7} K environment¹³, they must have high column densities of order $N_{\text{H}_2} \approx 10^{22-24} \text{ cm}^{-2}$ so as to maintain pressure support. The thermal pressure in the core of Abell 2597 is nearly three thousand times¹¹ greater than that for the Milky Way, however, which means the absorbing clouds may be much smaller.

The absorbers have optical depths that range from $0.1 \lesssim \tau_{\text{CO}(2-1)} \lesssim 0.3$. The physical resolution of the ALMA data is larger than the synchrotron background source, which means that the optical depth is likely contaminated by an unresolved, additive superposition of both emission and absorption within the beam. Compact, dense cold clouds are nevertheless likely to be optically thick, which may mean they eclipse the continuum source with an optical depth of unity but a small covering factor of roughly 0.2. Especially when considering beam contamination by emission, the covering factor cannot be known with certainty, as this depends on the unknown geometry of the absorbing and emitting regions within the ALMA beam.

This geometry can be constrained, however, given existing Very Long Baseline Array (VLBA) radio observations at extremely high spatial resolution¹⁵. These data resolve the 1.3 and 5 GHz radio continuum source down to scales of 25 parsecs, revealing a highly symmetric, 100 pc-scale jet about a bright radio core (Fig. 4c). Just as we have found in cold molecular gas, inflowing warmer atomic hydrogen gas (HI) has previously been found in absorption against this pc-scale jet, corroborating prior reports of inflowing atomic gas at lower spatial resolutions¹⁴. The inflow velocity of this gas matches that seen in our ALMA data. Remarkably, both the optical depth and linewidth of the warm atomic absorption signal varies dramatically across the jet, with a broad ($\sigma \approx 310 \text{ km s}^{-1}$) component cospatial with the core that is absent just $\sim 20 \text{ pc}$ to the northeast, where only a narrow ($\sigma \approx 50 \text{ km s}^{-1}$) HI line is found at the same redshift. This effectively requires the inflowing atomic gas to be confined within the innermost $\sim 100 \text{ pc}$ of the black hole, as gas further out would give rise to an unchanging absorption signal across the compact jet. The infall velocity is the same as that for the cold molecular clouds seen in CO(2-1) absorption, which means they most likely stem from the same spatial region, within tens of parsecs of the accreting black hole.

This is further supported by the ALMA data itself. In emission, all gas around $\sim +300 \text{ km s}^{-1}$ that is conceivably available to attenuate the continuum signal is confined to the innermost 2 kpc about the nucleus (Fig. 4a,b). The radial dependence of molecular cloud volume number density within this region is uncertain, but probably steeper than r^{-1} , and likely closer to r^{-2} (Fig. 4b). This means that the chances

of a random line of sight crossing will drop with increasing distance from the black hole. If the gas volume density goes as r^{-2} , a cloud 100 pc from the black hole is ten times more likely to cross our line of sight than a cloud at a galactocentric distance of 1 kpc. It would be exceedingly unlikely for three such clouds to cross our line of sight to the black hole were they spread over several kiloparsecs throughout the galaxy’s outskirts.

The data therefore serve as strong observational evidence for an inward-moving, clumpy distribution of molecular clouds within a few hundred parsecs of an accreting supermassive black hole. The infalling clouds are likely a few to tens of parsecs across and therefore massive (perhaps $10^{5-6} M_\odot$ each). If they are falling directly toward the black hole, rather than bound in a non-circular orbit that tightly winds around it, they could supply an upper-limit accretion rate on the order of ~ 0.1 to a few $M_\odot \text{ yr}^{-1}$, depending on the three dimensional distribution of infalling clouds. If most of the clouds are instead locked in non-circular orbits around the black hole, the fuelling rate would depend on the gas angular momentum, and the local supply of torques that might lessen it. Simulations suggest^{7,12} that such torques may be plentiful, as they predict a stochastic “rain” of thermal instabilities that condense from all directions around the black hole, promoting angular momentum cancellation via tidal stress and cloud-cloud collisions. Even highly elliptical cloud orbits should therefore be associated with significant inward radial motions. The clouds might fall onto the accretion disc itself, or into a clumpy rotating ring akin to the “torus” invoked in AGN unification models²⁷.

Cold accretion onto black holes has long been predicted by both theory and simulations⁵⁻¹⁰, but it has not been definitively observed in a manner so stripped of ambiguity regarding the clouds’ proximity to a black hole. While no observation of a single galaxy can prove this theoretical prediction to be definitively true, the combined ALMA and VLBA dataset for Abell 2597 enable a uniquely unambiguous observation of molecular clouds that are either directly associated with black hole growth, or are soon about to be. The result augments a small but growing set of previously published molecular absorption systems²⁸⁻³⁰ in which black hole proximity is less well constrained. These could nevertheless be used to inform future systematic searches for cold black hole accretion across larger samples. Multi-epoch observations with ALMA might reveal shifts in the absorption lines, confirming their close proximity, and resolving cold black hole accretion as it evolves through time.

Received 17 December 2015; accepted 16 March 2016.

1. McNamara, B. R. & Nulsen, P. E. J. Heating Hot Atmospheres with Active Galactic Nuclei. *Ann. Rev. Astron. Astrophys.* **45**, 117-175 (2007).
2. McNamara, B. R. & Nulsen, P. E. J. Mechanical feedback from active galactic nuclei in galaxies, groups and clusters. *New J. Phys.* **14**, 055023 (2012).
3. Fabian, A. C. Observational Evidence of Active Galactic Nuclei Feedback. *Ann. Rev. Astron. Astrophys.* **50**, 455-489 (2012).
4. Bondi, H. On spherically symmetrical accretion. *Mon. Not. R. Astron. Soc.* **112**, 195 (1952).
5. Pizzolato, F. & Soker, N. On the Nature of Feedback Heating in Cooling Flow Clusters. *Astrophys. J.* **632**, 821-830 (2005).
6. Voit, G. M., Donahue, M., Bryan, G. L. & McDonald, M. Regulation of star formation in giant galaxies by precipitation, feedback and conduction. *Nature* **519**, 203-206 (2015).
7. Voit, G. M., Bryan, G. L., O’Shea, B. W. & Donahue, M. Precipitation-regulated Star Formation in Galaxies. *Astrophys. J.* **808**, L30 (2015).
8. Sharma, P., McCourt, M., Quataert, E. & Parrish, I. J. Thermal instability and the feedback regulation of hot haloes in clusters, groups, and galaxies. *Mon. Not. R. Astron. Soc.* **420**, 3174-3194 (2012).
9. Gaspari, M., Ruszkowski, M. & Oh, S. P. Chaotic cold accretion on to black holes. *Mon. Not. R. Astron. Soc.* **432**, 3401-3422 (2013).
10. Li, Y. & Bryan, G. L. Modeling Active Galactic Nucleus Feedback in Cool-core Clusters: The Formation of Cold Clumps. *Astrophys. J.* **789**, 153 (2014).

ALMA Integrated $>3\sigma$ CO(2-1) emission

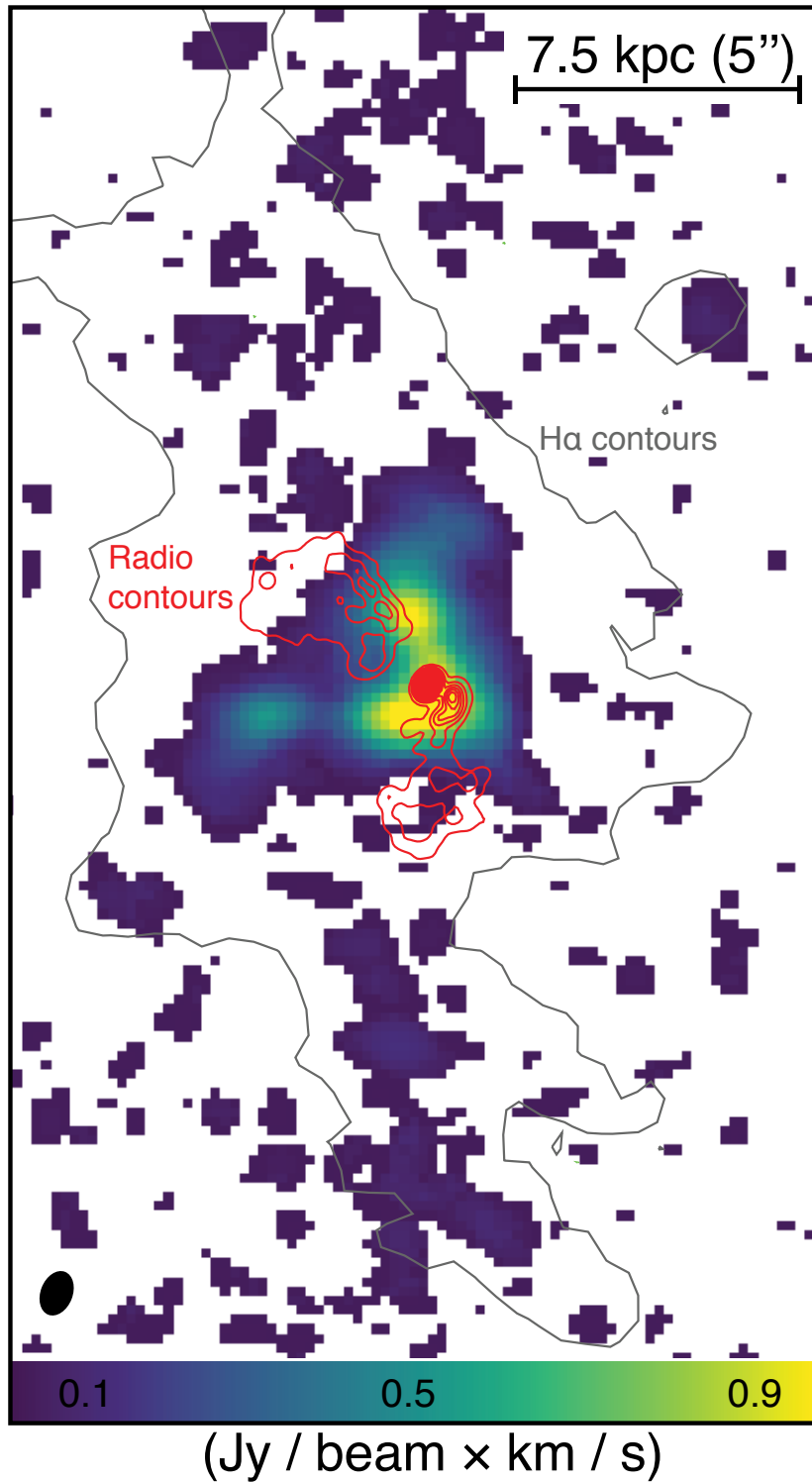


Figure 2 | ALMA observation of continuum-subtracted CO(2-1) emission in the Abell 2597 BCG. Emission is integrated from -600 to $+600$ km s^{-1} relative to the galaxy's systemic velocity. Channels are binned to 40 km s^{-1} . Only $\geq 3\sigma$ emission is shown. 8.4 GHz VLA radio contours are overlaid in black, and H α + [N II] contours outlining the rough boundary of the ionised nebula are shown in grey. The nebula is slightly larger than the grey contours suggest: emission outside of this boundary is still part of a smooth, fainter distribution of cold gas, cospatial with similarly faint emission in the optical.

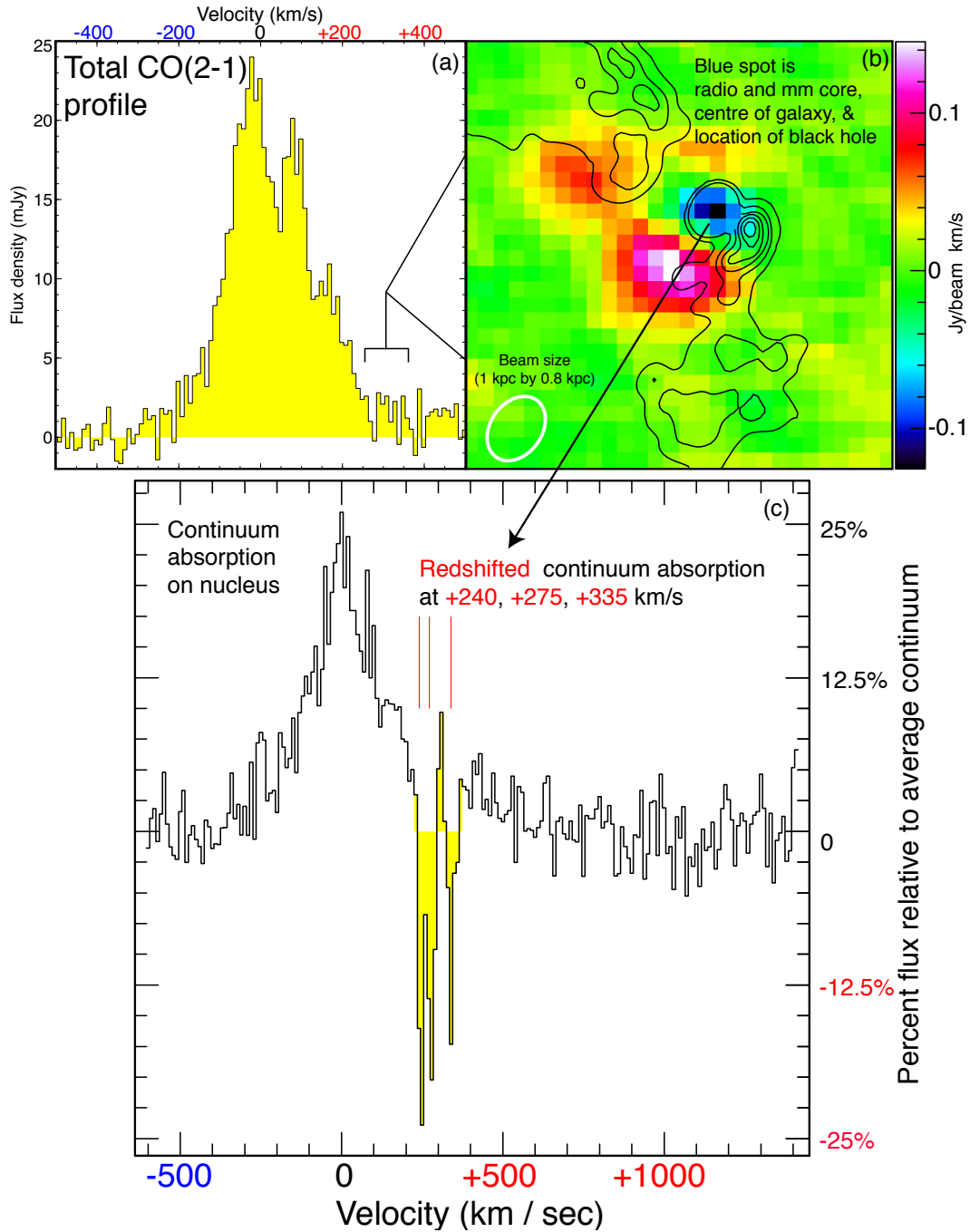


Figure 3 | “Shadows” cast by molecular clouds moving toward the supermassive black hole. (a) Continuum-subtracted ALMA CO(2-1) spectrum extracted from a central 10 kpc region. Brackets mark CO(2-1) emission shown in panel (b), where 8.4 GHz radio contours are overlaid. The central radio contours have been removed to aid viewing of the continuum absorption, seen as the blue/black spot of “negative” emission. (c) Continuum-subtracted CO(2-1) spectrum extracted from this region cospatial with the mm and radio core. Absorption lines are indicated in red.

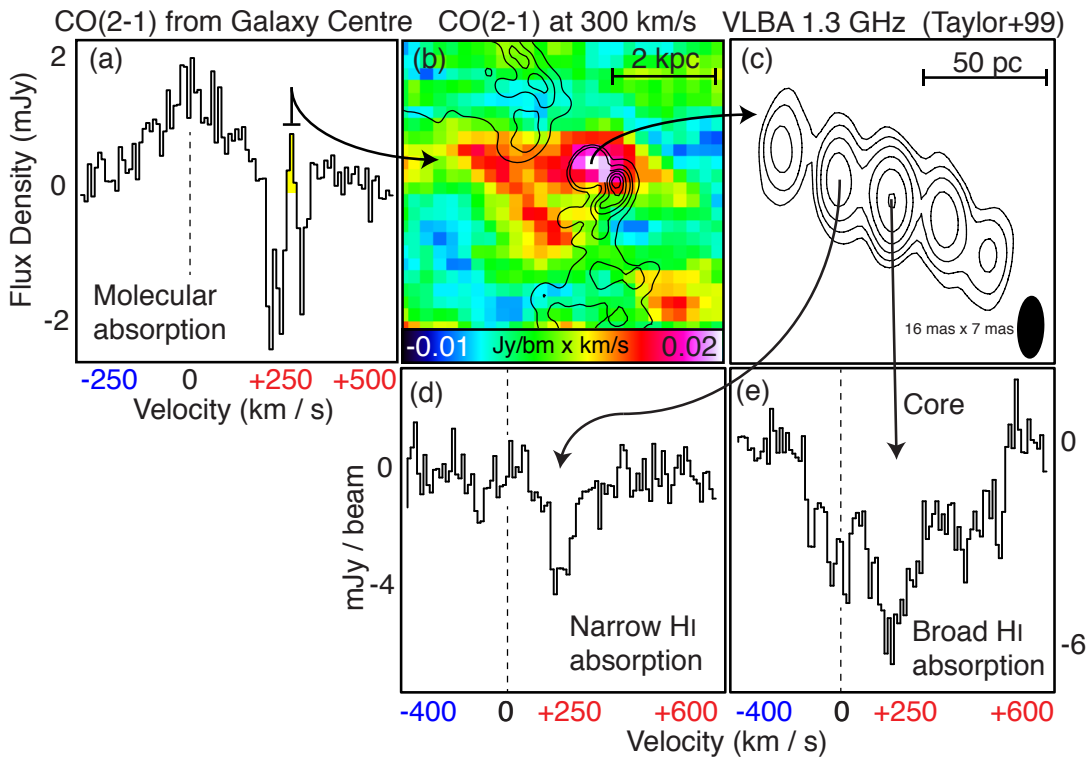


Figure 4 | Corroborating evidence that the inflowing molecular clouds must be in close proximity to the black hole. (a) CO(2-1) absorption spectrum from Fig. 3, with a region of emission at $\sim +300 \text{ km s}^{-1}$ marked in yellow. (b) Integrated emission from this region, showing that gas at $\sim +300 \text{ km s}^{-1}$ is confined to the innermost $\sim 2 \text{ kpc}$ of the galaxy. (c) 1.4 GHz radio continuum source from an archival VLBA observation¹⁷ with an extremely high physical resolution of ~ 25 parsecs by ~ 10 parsecs. (d,e) HI 21 cm absorption observed against this synchrotron jet. The signal varies dramatically over tens of parsec scales.

11. McNamara, B. R. *et al.* Discovery of Ghost Cavities in the X-Ray Atmosphere of Abell 2597. *Astrophys. J.* **562**, L149-L152 (2001).
12. Clarke, T. E., Sarazin, C. L., Blanton, E. L., Neumann, D. M. & Kassim, N. E. Low-Frequency Radio Observations of X-Ray Ghost Bubbles in A2597: A History of Radio Activity in the Core. *Astrophys. J.* **625**, 748-753 (2005).
13. Tremblay, G. R. *et al.* Multiphase signatures of active galactic nucleus feedback in Abell 2597. *Mon. Not. R. Astron. Soc.* **424**, 1026-1041 (2012).
14. Gaspari, M., Brighenti, F. & Temi, P. Chaotic cold accretion on to black holes in rotating atmospheres. *Astron. Astrophys.* **579**, A62 (2015).
15. Tremblay, G. R. *et al.* Residual cooling and persistent star formation amid active galactic nucleus feedback in Abell 2597. *Mon. Not. R. Astron. Soc.* **424**, 1042-1060 (2012).
16. O'Dea, C. P., Baum, S. A. & Gallimore, J. F. Detection of extended HI absorption toward PKS 2322-123 in Abell 2597. *Astrophys. J.* **436**, 669-677 (1994).
17. Taylor, G. B., O'Dea, C. P., Peck, A. B. & Koekemoer, A. M. HI Absorption toward the Nucleus of the Radio Galaxy PKS 2322-123 in A2597. *Astrophys. J.* **512**, L27-L30 (1999).
18. O'Dea, C. P., Baum, S. A., Mack, J., Koekemoer, A. M. & Laor, A. *Hubble Space Telescope* STIS Far-Ultraviolet Observations of the Central Nebulae in the Cooling-Core Clusters A1795 and A2597. *Astrophys. J.* **612**, 131-151 (2004).
19. Oonk, J. B. R., Hatch, N. A., Jaffe, W., Bremer, M. N. & van Weeren, R. J. Far-ultraviolet emission in the A2597 and A2204 brightest cluster galaxies. *Mon. Not. R. Astron. Soc.* **414**, 2309-2336 (2011).
20. Tremblay, G. R. *et al.* Far-ultraviolet morphology of star-forming filaments in cool core brightest cluster galaxies. *Mon. Not. R. Astron. Soc.* **451**, 3768-3800 (2015).
21. Salomé, P. *et al.* A very extended molecular web around NGC 1275. *Astron. Astrophys.* **531**, A85 (2011).
22. Jaffe, W., Bremer, M. N. & Baker, K. HII and H₂ in the envelopes of cooling flow central galaxies. *Mon. Not. R. Astron. Soc.* **360**, 748-762 (2005).
23. Salomé, P. *et al.* Cold molecular gas in the Perseus cluster core. Association with X-ray cavity, H α filaments and cooling flow. *Astron. Astrophys.* **454**, 437-445 (2006).
24. Smith, E. P., Heckman, T. M., & Illingworth, G. D. Stellar dynamics of powerful radio galaxies. *Astrophys. J.* **356**, 399-415 (1990).
25. Larson, R. B. Turbulence and star formation in molecular clouds. *Mon. Not. R. Astron. Soc.* **194**, 809-826 (1981).
26. Solomon, P. M., Rivolo, A. R., Barrett, J. & Yahil, A. Mass, luminosity, and line width relations of Galactic molecular clouds. *Astrophys. J.* **319**, 730-741 (1987).
27. Urry, C. M. & Padovani, P. Unified Schemes for Radio-Loud Active Galactic Nuclei. *Publ. Astron. Soc. Pac.* **107**, 803U (1995).
28. Wiklind, T. & Combes, F. Molecular absorption and its time variations in Centaurus A. *Astron. Astrophys.* **324**, 51-64 (1997).
29. Espada, D. *et al.* Disentangling the Circumnuclear Environs of Centaurus A. II. On the Nature of the Broad Absorption Line. *Astrophys. J.* **720**, 666-678 (2010).
30. David, L. P. *et al.* Molecular Gas in the X-Ray Bright Group NGC 5044 as Revealed by ALMA. *Astrophys. J.* **792**, 94 (2014).
31. Voit, G. M. & Donahue, M. A Deep Look at the Emission-Line Nebula in Abell 2597. *Astrophys. J.* **486**, 242+ (1997).
32. Bolatto, A. D., Wolfire, M. & Leroy, A. K. The CO-to-H₂ Conversion Factor. *Ann. Rev. Astron. Astrophys.* **51**, 207-268 (2013).
33. McNamara, B. R. *et al.* A 10^{10} Solar Mass Flow of Molecular Gas in the A1835 Brightest Cluster Galaxy. *Astrophys. J.* **785**, 44 (2014).
34. Russell, H. R. *et al.* Massive Molecular Gas Flows in the A1664 Brightest Cluster Galaxy. *Astrophys. J.* **784**, 78 (2014).

Acknowledgements This paper makes use of the following ALMA data: ADS/JAO.ALMA#2012.1.00988.S. ALMA is a partnership of ESO (representing its member states), NSF (USA) and NINS (Japan), together with NRC (Canada) and NSC and ASIAA (Taiwan), in cooperation with the Republic of Chile. The Joint ALMA Observatory is operated by ESO, AUI/NRAO and NAOJ. We are grateful to the European ALMA Regional Centres, particularly those in Garching and Manchester, for their dedicated end-to-end support of data associated with this paper. We thank Prof. Richard Larson for discussions. G.R.T. acknowledges support from the National Aeronautics and Space Administration (NASA) through Einstein Postdoctoral Fellowship Award Number PF-150128, issued by the Chandra X-ray Observatory Center, which is operated by the Smithsonian Astrophysical Observatory for and on behalf

of NASA under contract NAS8-03060. F.C. acknowledges the European Research Council (ERC) for the Advanced Grant Program #267399-*Momentum*. B.R.M. is supported by a generous grant from the Natural Sciences and Engineering Research Council of Canada. T.A.D. acknowledges support from a Science and Technology Facilities Council (STFC) Ernest Rutherford Fellowship. A.C.E. acknowledges support from STFC grant ST/L00075X/1. A.C.F. and H.R.R. acknowledge support from ERC Advanced Grant Program #340442-*Feedback*. M.N.B. acknowledges funding from the STFC. Basic research in radio astronomy at the Naval Research Laboratory is supported by 6.1 Base funding.

Author Contributions G.R.T. was principal investigator on the original proposal, performed the data analysis, and wrote the paper. J.B.R.O., T.A.D., R.G.M., and A.M. were substantially involved in planning both scientific and technical aspects of the proposal, while T.A.D. and R.G.M. contributed ALMA data reduction and analysis expertise once the data were obtained. J.B.R.O., F.C., and P.S. invested substantial time in analysis of the data. Substantial scientific feedback was also provided over many months by F.C., J.B.R.O., C.P.O., S.A.B., G.M.V., M.D., B.R.M., M.A.M., T.E.C., H.R., A.C.E. and A.C.F., while all other co-authors discussed the results and commented on the manuscript.

Author Information Reprints and permissions information is available at www.nature.com/reprints. The authors declare no competing financial interests. Readers are welcome to comment on the online version of this article. Correspondence and requests for materials should be addressed to G.R.T. (email: grant.tremblay@yale.edu).

METHODS

Observations, Data Reduction, and Analysis. The new ALMA data presented in this paper were obtained in Cycle 1 with the use of 29 operational antennae in the 12m Array. ALMA’s Band 6 heterodyne receivers were tuned to a frequency of 213 GHz, sensitive to the $J = 2 - 1$ rotational line transition of carbon monoxide at the redshift of the Abell 2597 BCG ($z = 0.0821$). The ALMA correlator, set to Frequency Division Mode (FDM), delivered a bandwidth of 1875 MHz (per baseband) with a 0.488 MHz channel spacing, for a maximum spectral resolution of ~ 2 km s^{-1} . One baseband was centered on the CO(2-1) line, while the other three sampled the local continuum. Maximum antenna baselines extended to ~ 1 km, delivering an angular resolution at 213 GHz of $\sim 0''.7$ within a $\sim 28''$ primary beam (field of view). ALMA observed the Abell 2597 BCG for a total of ~ 3 hours over three separate scheduling blocks executed between 17-19 November 2013. The planet Neptune and quasars J2258-2758 and J2331-1556 were used for amplitude, flux, and phase calibration. The data were reduced using CASA version 4.2 with calibration and imaging scripts kindly provided by the ALMA Regional Centres (ARCs) in both Garching, Germany, and Manchester, UK. Beyond the standard application of the phase calibrator solution, we iteratively performed self-calibration of the data using the galaxy’s own continuum, yielding a $\sim 14\%$ decrease in RMS noise to a final value of 0.16 mJy per $0''.715 \times 0''.533$ beam per 40 km s^{-1} channel. There is effectively no difference in CO(2-1) morphology between the self-calibrated and non-self-calibrated cubes. Measurement sets were imaged using “natural” visibility weighting and binning to either 5 km s^{-1} , 10 km s^{-1} or 40 km s^{-1} , as indicated in the figure captions. The figures presented in this paper show only continuum-subtracted, pure CO(2-1) line emission. The rest-frame 230 GHz continuum observation is dominated by a bright (13.6 mJy) point source associated with the AGN (detected at $\gtrsim 400\sigma$), serving as the bright “backlight” against which the continuum absorption features presented in this Letter were observed. The continuum data also features compact (~ 5 kpc) extended emission at $\sim 10\sigma$ that extends along the galaxy’s dust lane, to be discussed in a forthcoming paper.

Adoption of a systemic velocity. Interpretation of gas motions relative to the stellar component of a galaxy requires adoption of a systemic (stellar) velocity to be used as a “zero point” marking the transition from blue- to redshift. All CO(2-1) line velocities discussed in this Letter are set relative to 213.04685 GHz, where observed CO(2-1) emission peaks. This frequency corresponds to $^{12}\text{CO}(2-1)$ (rest-frame 230.538001 GHz) at a redshift of $z = 0.0821$. This redshift is consistent, conservatively within ± 60 km s^{-1} , with every other available multiwavelength tracer of the galaxy’s systemic velocity, including prominent Ca II H, K, and G-band absorption features¹⁶ that directly trace the galaxy stellar component, the redshift of all optical emission lines³¹, as well as a broad (FWHM ~ 412 km s^{-1}) H α absorption component¹⁶ at the optical emission and absorption line redshift. It is also consistent, within ± 60 km s^{-1} , with a cross-correlation of emission and absorption lines using galaxy template spectra¹⁵, as well as with all other published reports of the galaxy’s systemic velocity (found, e.g., within the HyperLeda database). We are therefore certain that the reported redshift of the absorption features discussed in this letter indeed corresponds to real motion relative to the galaxy’s stellar component. Without caveat or ambiguity, the absorbing cold clouds are moving *into* the galaxy at roughly $\sim +300$ km s^{-1} .

Mass Estimates. All molecular gas masses estimated in this letter adopt the following relation³²:

$$M_{\text{mol}} = \frac{1.05 \times 10^4}{3.2} \left(\frac{X_{\text{CO}}}{2 \times 10^{20} \frac{\text{cm}^{-2}}{\text{K km s}^{-1}}} \right) \left(\frac{1}{1+z} \right) \left(\frac{S_{\text{CO}\Delta\nu}}{\text{Jy km s}^{-1}} \right) \left(\frac{D_L}{\text{Mpc}} \right)^2 M_{\odot}, \quad (1)$$

where $S_{\text{CO}\Delta\nu}$ is the emission integral for CO(1-0) (effectively the total CO(1-0) flux over the region of interest), z is the galaxy redshift ($z = 0.0821$), and D_L its luminosity distance (373.3 Mpc), for which we assume a flat Λ CDM model wherein $H_0 = 70$ km s^{-1} Mpc $^{-1}$, $\Omega_M = 0.3$, and $\Omega_{\Lambda} = 0.7$. This mass estimate most critically relies on an assumption of the CO-to-H $_2$ conversion factor³² X_{CO} . In this Letter we assume the average Milky Way value of $X_{\text{CO}} = 2 \times 10^{20}$ cm $^{-2}$ (K km s^{-1}) $^{-1}$ and a CO(2-1) to CO(1-0) flux density ratio of 3.2. Other authors have provided extensive discussion of these assumptions as they pertain to cool core BCGs^{30,33,34}. Scientific conclusions in this paper are largely insensitive to choice of X_{CO} .

A single gaussian fit to the CO(2-1) spectrum extracted from an aperture containing all detected emission yields an emission integral of $S_{\text{CO}\Delta\nu} = 4.2 \pm 0.4$ Jy km s^{-1} with a line FWHM of 252 ± 14 km s^{-1} , corresponding to a total molecular hydrogen (H $_2$) gas mass of $M_{\text{H}_2} = (1.80 \pm 0.19) \times 10^9 M_{\odot}$. This is very close to the previously reported¹³ mass, based on an IRAM 30m CO(2-1) observation, of $(1.8 \pm 0.3) \times 10^9 M_{\odot}$. This comparison is not one-to-one, as the mass from the IRAM 30m observation was computed within a beam size of $11''$ (rather than $28''$ for the ALMA data), and used a CO(2-1)/CO(1-0) flux ratio of 4 (rather than 3.2, as we use here). These differences are minor, particularly because nearly all of the CO(2-1) emission detected by ALMA is found within the central $11''$ size of the IRAM 30m beam. It is therefore safe to say that our ALMA observation has detected nearly all emission that was detected in the single-dish IRAM 30m observation, and that very little extended emission has been “resolved out”.

Estimating physical properties of the redshifted absorbing gas. We have estimated a rough upper-limit size of the absorbing clouds assuming the widely-adopted Larson et al.²⁵ and Solomon et al.²⁶ size-linewidth relation for molecular clouds in the Milky Way (namely, the Solomon et al. 1987 fit),

$$\sigma = (1.0 \pm 0.1) S^{0.5 \pm 0.05} \text{ km s}^{-1}, \quad (2)$$

where σ is the velocity line-width of the cloud and S is the diameter of the cloud in parsecs.

A measured absorber linewidth of $\sigma \sim 6$ km s^{-1} would then correspond to a size of ~ 36 pc. As noted in the main text of the Letter, the thermal pressure in the Abell 2597 Brightest Cluster Galaxy is likely up to three orders of magnitude higher than that for the Milky Way, so it is likely that the above relation does not apply. A higher ambient pressure implies higher

compression and therefore smaller cloud size, so the above estimate should, at best, be considered a very rough upper-limit. The main lesson to take away from this exercise is that the absorbing clouds are likely physically compact (i.e. a few to tens of parsecs in diameter, rather than hundreds of pc).

The three clouds are separated from one another by $\sim 45 - 60 \text{ km s}^{-1}$ in velocity space, which means they are unlikely to be closely bound satellites of one another. Instead, it is more likely that they represent three random points along a radial distribution of clouds.

If the absorbers are in virial equilibrium, their masses M_{cloud} can be roughly estimated by applying the virial relation,

$$M_{\text{cloud}} \approx \frac{R_{\text{cloud}} \sigma^2}{G} \approx \frac{20 \text{ pc} \times (6 \text{ km/s})^2}{4.302 \times 10^{-3} \text{ pc } M_{\odot}^{-1} (\text{km/s})^2} \approx 1.7 \times 10^5 M_{\odot}, \quad (3)$$

where R_{cloud} is the cloud radius (as roughly estimated above) and σ is its velocity dispersion (also as above).

CO(2-1) optical depths for the absorbers were estimated by assuming that

$$I_{\text{total}} = I_{\text{continuum}} e^{-\tau_{\text{CO}(2-1)}}, \quad (4)$$

where I_{total} and $I_{\text{continuum}}$ are the integrated intensities of the total (line plus continuum) and continuum-only signals, respectively, and $\tau_{\text{CO}(2-1)}$ is the optical depth of the CO(2-1) absorption feature.

The stellar velocity dispersion of the BCG² is $\sigma = 220 \pm 19 \text{ km s}^{-1}$. Under the assumption of an isothermal sphere, the circular velocity should be $\sim 300 \text{ km s}^{-1}$, (i.e., $\sqrt{2}\sigma$) which is roughly the line of sight velocity of the absorption features. The redshift of the absorption features is a significant fraction of this, which means they could be on a purely radial orbit (though their transverse velocity cannot be known with this single observation).

If our line of sight is representative, and therefore a ‘‘pencil beam’’ sample of a three-dimensional spherical distribution of clouds, the total mass of cold gas contained within this distribution should go roughly as

$$M \approx 10^9 M_{\odot} \times f_c \times \left(\frac{r}{1 \text{ kpc}} \right)^2 \times \left(\frac{N_{\text{H}}}{10^{22} \text{ cm}^{-2}} \right) \quad (5)$$

where f_c is the covering factor and r is the radius of an imaginary thin spherical shell of molecular gas with column density N_{H} . If such a shell had a covering factor of 1, a radius of 1 kpc, and a column density of 10^{22} cm^{-2} , then the total mass of molecular hydrogen contained within that shell would be roughly one billion solar masses. A column density in excess of 10^{22} requires this distribution to be contained within a sphere of radius $\ll 1$ kpc, lest the total mass of molecular hydrogen in the galaxy be violated. If the characteristic column density is 10^{23} cm^{-2} , for example, this mass must be contained within a sphere of radius 300 pc, or else its total mass would exceed the $\sim 1.8 \times 10^9 M_{\odot}$ present in the system.

Code, software, and data availability. The raw ALMA data used in this Letter are publicly available at the [ALMA Science Archive](#) (search for project code 2012.1.00988.S). Codes that we have written to both reduce and analyse the ALMA data have been made publicly available [here](#). Reduction of the data as well as some simple modeling (e.g., fitting of Gaussians to lines) was performed using routines included in CASA version 4.2, available [here](#).